Relevance of Substrate Temperature and Ga Kinetics on Mg Doping in GaN by Plasma-Assisted Molecular Beam Epitaxy

Elçin Akar, Adeline Grenier, Anne-Marie Papon, Audrey Jannaud, Martien Ilse den Hertog, Eva Monroy

CRYSTAL GROWTH & DESIGN

pubs.acs.org/crystal

Article

Relevance of Substrate Temperature and Ga Kinetics on Mg Doping in GaN by Plasma-Assisted Molecular Beam Epitaxy

Elçin Akar,* Adeline Grenier, Anne-Marie Papon, Audrey Jannaud, Martien Ilse den Hertog, and Eva Monroy

Cite This: https://doi.org/10.1021/acs.cgd.4c00777

Read Online

ACCESS | Metrics & More | Article Recommendations | Supporting Information

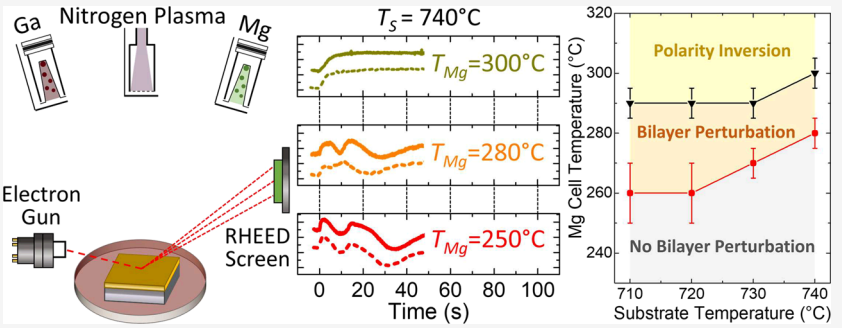

ABSTRACT: This study investigates the influence of substrate temperature and III/V ratio on the synthesis of Mg-doped GaN layer using plasma-assisted molecular beam epitaxy. We demonstrate that optimum growth conditions are the result of a delicate balance between substrate temperature, Mg flux, and III/V ratio. At low substrate temperatures, where Ga desorption from the growing surface is negligible, a pronounced self-compensation effect linked to polarity inversion significantly reduces net acceptor concentration at relatively low Mg cell temperatures. Increasing the substrate temperature allows for higher Mg fluxes, enhancing the net acceptor concentration before reaching the collapse due to polarity inversion. Detailed analysis of Ga desorption during growth interruptions highlights the susceptibility of the Ga bilayer to perturbations under varying Mg fluxes, attributed to the replacement of Ga adatoms by Mg. We demonstrate that the polarity inversion is triggered when the Ga bilayer is reduced to a monolayer, either by the influence of the Mg flux or by a reduction of the Ga flux. This study demonstrates that maintaining a substantial Ga excess, within the bilayer regime and close to the Ga droplet accumulation threshold, is vital for preventing polarity inversion.

INTRODUCTION

Efforts to improve the p-type conductivity of GaN keep attracting interest as a key element to improve the performance of light-emitting diodes,[1] lasers,[2] avalanche photodiodes,[3] etc. Magnesium (Mg) is the primary p-type dopant employed as an acceptor in GaN. However, challenges arise due to its high activation energy (150 to 250 meV), tendency for self-compensation, and the generation of inversion domains. To achieve a hole concentration approaching 10^{18} cm^{-3}, it is necessary to introduce a concentration of Mg in the range 10^{19} to 10^{20} cm^{-3}, which leads to a decline of the hole mobility and promotes the generation of structural defects. Additionally, self-compensation appears for high Mg concentration, associated with the creation of V_N−Mg_{Ga} complexes,[4] enhanced incorporation of point defects,[5] or simply generation of N vacancies.[6,7]

Numerous studies have explored the optimization of Mg doping in the literature through various epitaxy methods like metalorganic chemical vapor deposition (MOCVD) and molecular beam epitaxy (MBE).[8] Unlike NH_3-MBE, plasma-assisted MBE (PAMBE) offers specific advantages since it prevents issues related to hydrogen passivation. Therefore, in PAMBE-grown samples, there is no requirement for a post-annealing process to activate the acceptors. Additionally, the reduced growth temperature facilitates higher dopant incorporation, which has motivated the use of this technique as a complement to MOCVD to optimize the tunnel contact of light-emitting devices.[9−11] To overcome aforementioned difficulties related to Mg doping, different approaches have been proposed, such as metal modulated epitaxy[12,13] or using indium as a surfactant during growth.[14−16] Still, the dominant approach is to tune the growth conditions, namely, substrate temperature, Ga/N ratio, and Mg flux, to enhance the incorporation of Mg in the grown epilayers.

If we focus on the substrate temperature, using the standard growth temperature of non-intentionally doped GaN as a

Received: June 7, 2024
Revised: August 5, 2024
Accepted: August 5, 2024

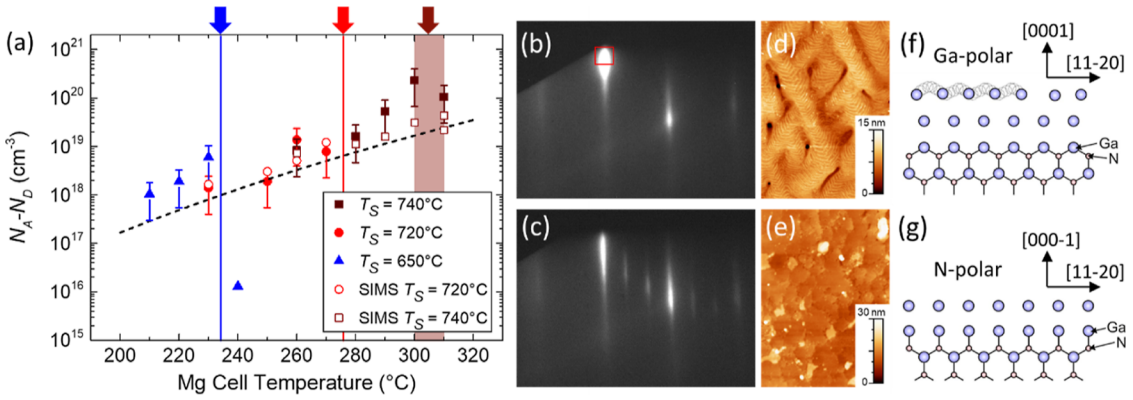

Figure 1. (a) Variation of the net acceptor concentration as a function of the Mg cell temperature extracted from $C-V$ measurements. SIMS measurements performed in reference samples grown at T_S = 720 and 740 °C are superimposed. The figure regroups samples grown at three substrate temperatures. The top arrows and vertical lines (band, in the case of 740 °C) indicate the polarity inversion threshold. The dashed line is an eye guide to represent the Mg flux trend extracted from measurements of beam equivalent pressure of Mg. (b) RHEED pattern of Ga-polar GaN viewed along the ⟨11−20⟩ azimuth. (c) RHEED pattern of N-polar GaN viewed along ⟨11−20⟩, displaying a characteristic 3 × 3 reconstruction. (d) Typical AFM image of Ga-polar GaN:Mg. (e) Typical AFM image of GaN:Mg after polarity inversion. Schematic representation of (f) Ga-polar and (g) N-polar GaN during PAMBE growth.

reference (around 700 °C), lowering the substrate temperature results in an increase of Mg incorporation in GaN,[17−20] which suggests that the desorption of Mg from the substrate is important in that substrate temperature range. Then, reports suggest that the III/V ratio has no significant effect on Mg incorporation but exerts a notable influence on the surface morphology of the fabricated epilayers. When the III/V ratio is greater than 1, the Mg-doped GaN layers exhibit p-type conductivity with a smooth surface.[19,21] Conversely, a decrease in the III/V ratio results in a significant increase in surface roughness and a decrease in the conductivity. Finally, Mg incorporation should increase linearly with the Mg flux.[18,21,22] To attain a high Mg concentration (>10^{19} cm^{-3}), a comprehensive examination of these parameters should be conducted to determine the optimal growth conditions.

Another crucial aspect of Mg doping is the risk of polarity inversion. Epitaxial layers fabricated via PAMBE are generally grown along the [0001] crystallographic axis, i.e., with Ga polarity. During growth, Mg atoms tend to segregate within the crystal structure of grown GaN layers, which can lead to inversion from Ga polarity to N polarity.[23] Inversion domains appear as inverted pyramidal domains in MOCVD and as columnar domains in MBE.[24−26] While the nitrogen polarity of GaN might be interesting for certain applications,[27,28] the occurrence of polarity inversion in Mg-doped GaN layers appears to be associated with unfavorable outcomes. Samples undergoing polarity inversion display high dislocation density, and some reports suggest a notable reduction in Mg incorporation.[18,20,29] Overall, p-type doping of GaN with Mg continues to pose challenges, necessitating further in-depth analysis and investigation.

In this study, we propose a growth window to increase the Mg concentration and net acceptor concentration in PAMBE-grown Mg-doped GaN. High Mg concentrations (>10^{19} cm^{-3}) are achieved at a substrate temperature that is around 40 °C higher than our standard growth temperature for undoped GaN. Furthermore, an investigation into the growth kinetics at elevated substrate temperatures was carried out to analyze the impact of Mg on the adsorbed Ga excess that is required to obtain planar layers. Using reflection high-energy electron diffraction (RHEED), we have established a correlation between substrate temperature, Mg flux, Ga/N flux ratio, and polarity inversion.

EXPERIMENTAL SECTION

The GaN samples under study were fabricated by PAMBE on commercial 4 μm-thick GaN:Si-on-sapphire templates with [Si] ≈ 1.7 × 10^{18} cm^{-3}. The substrates were mounted with indium on a molybdenum sample holder. The nitrogen plasma source was operated at 300 W radio frequency power with a 1 sccm flow rate, which leads to an N-limited growth rate of 0.59 ML/s. In the case of p−n junctions, the growth started with the deposition of an n-type GaN layer doped with [Si] = 3 × 10^{19} cm^{-3}. Then, we deposited a 200 nm-thick Mg-doped layer.

In our experiments, the growth temperature was varied in the range of 650 to 750 °C. The calibration of the substrate temperature for synthesizing GaN layers was based on Ga desorption time values, measured using RHEED.[30] The quantitative calibration of the substrate temperature is performed after a maintenance of the epitaxy reactor to be sure that the pyrometer window is not metalized (there is a drift of the measurement with time due to Ga deposition). At that point, we use RHEED oscillations to measure the Ga desorption time from the GaN surface after the deposition of 2 atomic layers of Ga, corresponding to each real temperature value recorded by the pyrometer. The Ga desorption process is thermally activated and provides a precise measurement (±5 °C) of the surface temperature in the range of 700−750 °C. Then, during the growth, the substrate temperature is regulated using a thermocouple, which is not in direct contact with the substrate. Therefore, there is an offset between the thermocouple reading and the real substrate temperature. The real substrate temperature is obtained for each sample by measuring the Ga desorption time by RHEED and comparing the result with the temperature measured with a pyrometer during the calibration process. In the case of temperatures below 700 °C, the desorption of Ga is too slow. In the range of 600−700 °C, we use the desorption time of indium as a temperature reference, as described in detail in the work of Valdueza-Felip et al.[31]

To measure the net acceptor concentration, samples were processed to fabricate mesa devices with a size of 200 × 200 μm^2. The mesa etching of GaN was performed using inductively coupled plasma-reactive ion etching (ICP-RIE) with BCl_3/Cl_2 (30/10 sccm) chemistry with a pressure in the chamber of 10 mTorr, a radio frequency power of 30 W, and an ICP power of 100 W. Subsequently, both p and n-type GaN were contacted via optical lithography and electron beam evaporation. Capacitance−voltage ($C-V$) measurements were performed by using an Agilent 4284A LCR meter connected to a probe station. The probe signal was 50 mV in amplitude with a frequency of 10

https://doi.org/10.1021/acs.cgd.4c00777
Cryst. Growth Des. XXXX, XXX, XXX−XXX

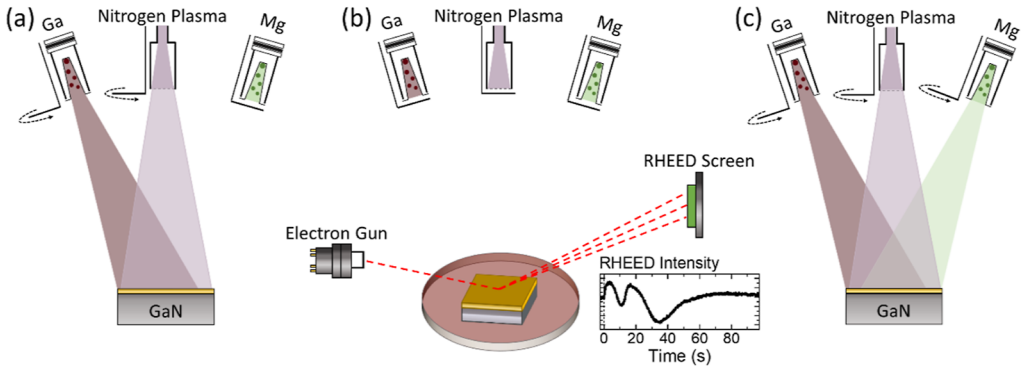

Figure 2. (a) Schematic view of the PAMBE growth of n.i.d. GaN (only Ga and N cells are open). (b) Schematic view of the RHEED characterization during a growth interruption (all cells are shuttered) with an example of RHEED intensity transient from Ga desorption. (c) Growth of GaN:Mg with Mg cell open together with Ga and N cells.

kHz. Measurements confirmed that the measured impedance was stable as a function of frequency in the range below 100 kHz. The quantification of Mg incorporation on the samples grown at T_S = 720 °C and T_S = 740 °C was carried out through secondary ion mass spectrometry (SIMS), using O_2^+ as primary ion beam and scanning an area of 175 × 175 μm.

The surface morphology of the samples was assessed using atomic force microscopy (AFM) using a Bruker Dimension Icon system equipped with Bruker TESPA-V2 tips and operated in tapping mode.

RESULTS

Effect of the Substrate Temperature. To assess the effect of the substrate temperature, T_S, we synthesized three series of samples grown at T_S = 650, 720, and 740 °C. Note that the desorption of Ga is negligible at T_S = 650 °C, and T_S = 720 °C is the typical growth temperature for GaN in our system (for reproduction, see the Ga desorption rate measured by RHEED at 720 °C in ref 30). For each series, we examine the evolution of the net acceptor concentration, $N_A - N_D$, as a function of the Mg cell temperature calculated from $C-V$ measurements using

$$N_A - N_D = \frac{2}{A^2 q \varepsilon_0 \varepsilon_s \mathrm{d}(C^{-2})/\mathrm{d}V} \quad (1)$$

where A is the area of the measured device, q is the elementary charge, ε_0 is the permittivity of vacuum, and ε_s is the dielectric constant of the material.

Within each series, the rise in Mg cell temperature, T_{Mg}, leads to a higher net acceptor concentration (see Figure 1a). Specifically, in the case of growth at 650 °C, $N_A - N_D$ collapses at T_{Mg} = 240 °C, indicating a sudden self-compensation effect, which has been previously reported by other groups.[5,32] Increasing the substrate temperature allows a further increase in T_{Mg} to attain higher values of $N_A - N_D$ before collapse occurs. The arrows on top of the graph depicted in Figure 1a indicate the T_{Mg} values for which collapse is highly probable at a given substrate temperature. In the case of T_S = 740 °C, we have detected reproducibility issues in the range of T_{Mg} = 300−310 °C. To verify that the result of $C-V$ measurements is consistent with the Mg concentration in the samples, we conducted SIMS measurements on GaN:Mg reference samples grown at T_S = 720 and 740 °C. The results are superimposed in Figure 1a using hollow symbols. The trend is similar, but there are variations that become more important at higher substrate temperature, which points out the sensibility of Mg incorporation to the growth conditions. Indeed, samples grown at higher substrate temperatures are more prone to temperature gradients during the growth.

The sudden drop in net acceptor concentration can also be associated with a polarity inversion, which has been observed previously in Mg-doped GaN layers.[18,20,23,33−35] Despite its recurrence during planar growth of GaN:Mg layers, the underlying mechanisms are not well understood, but seem associated with the replacement of Ga by Mg in the metallic adlayer that forms at the growth front.[36] During growth, RHEED patterns do not reveal any sign of polarity inversion. Nevertheless, the dominant polarity of the final layers can be readily verified in situ upon cooling the sample. Specifically, flat layers with Ga polarity present 1 × 1 (or 2 × 2 under nitrogen flux) reconstruction (see Figure 1b), in contrast to N-polar GaN, which is characterized by a distinctive 3 × 3 reconstruction (see Figure 1c). Ex situ, the two polarities present different sample morphology (see AFM images in Figure 1d,e)[37] and different reactivity in KOH solutions.[38] Ga-polar GaN demonstrates a step-flow growth pattern with atomic terraces, attributed to the presence of the Ga bilayer during growth.[39] On the contrary, the surface morphology undergoes a complete transformation, with increased roughness, when polarity inversion occurs.[40] The polarity inversion is expected to occur either as faceted boundaries with a pyramidal shape[24−26] or as columnar-like domains[23] which propagate through the Mg-doped GaN layer. We observed the latter phenomenon in the PAMBE-grown Mg-doped GaN layer. The sample from Figure 1e was observed by scanning electron microscopy (SEM) and bright-field scanning transmission electron microscopy (BF-STEM) and is given as Supporting Information, Figure S1. The polarity inversion appeared as randomly distributed columnar-like domains, commencing at the interface between the Mg-doped GaN and the Si-doped GaN.

Therefore, polarity inversion emerges as a critical concern, not only due to the structural degradation but also to the enhanced incorporation of pollutants linked to the N polarity.[41,42] In particular, enhanced levels of oxygen can impede obtaining p-type conductivity. Hence, circumventing polarity inversion during the growth of Mg-doped GaN layers is imperative, and it requires precise control over growth conditions.

Effect of the Mg Flux: Threshold of Polarity Inversion. The polarity inversion is assumed to be associated with a saturation of the surface with Mg atoms.[18,33,35] Therefore, in the first stage, we address here the effect of the Mg flux on the polarity inversion. With this purpose, we have designed an experiment to detect by RHEED the onset of the polarity

https://doi.org/10.1021/acs.cgd.4c00777
Cryst. Growth Des. XXXX, XXX, XXX−XXX

inversion, relying on the difference of Ga wetting between (0001) and (000−1) planes.[43]

Epitaxial layers grown by PAMBE with Ga polarity are generally grown under conditions of Ga excess. This regime facilitates the growth dynamics that enable the formation of a laterally contracted Ga bilayer on the growing surface.[44,45] Such a configuration yields a smooth epitaxial layer surface, attributed to step-flow growth, which is promoted by the enhanced adatom mobility and the decrease in the Ehrlich−Schwoebel barrier at the atomic step edges[46] (see Figure 1f). In contrast, when dealing with GaN with N polarity under Ga-rich conditions, the metal excess arranges into one single atomic layer of gallium, as depicted in Figure 1g, instead of a bilayer, prior to its transformation into Ga droplets.[43] This distinction suggests that Ga and N polarity can be differentiated by monitoring the desorption of Ga during a growth interruption. However, the experiment must consider that Mg fluxes below the polarity inversion threshold may significantly perturb the Ga kinetics during growth.[21]

To assess the use of RHEED to identify the threshold of polarity inversion, we used a non-intentionally doped (n.i.d.) Ga-polar GaN substrate. Experiments were performed with an optimized Ga/N ratio to ensure the formation of a laterally contracted Ga bilayer. Within the range of Ga fluxes that lead to bilayer formation, we selected a flux value slightly below the Ga accumulation point (Ga cell temperature about 3 °C below the droplet formation regime).[21] During the experiments, we deposited n.i.d. GaN using a Ga effusion cell and the N plasma cell, as represented schematically in Figure 2a. Once stable conditions were reached, we could get access to the Ga coverage of the surface by performing a growth interruption (Figure 2b) and recording the RHEED intensity transient due to the desorption of the Ga that accumulated at the surface. This reference transient was then compared with that obtained after the growth of GaN:Mg (configuration in Figure 2c), using various temperatures of the Mg cell. To ensure consistency, the sample was kept in the same position throughout the whole experiment (no rotation) and RHEED transients were consistently recorded from the same area of the specular reflection, marked by a red square in Figure 1b.

The first experiment, performed at a substrate temperature of 740 °C, is described in Figure 3a,b. Initially, an n.i.d. GaN layer of about 100 nm was deposited on the GaN substrate to hinder impurity diffusion from the substrate to the grown layers and to calibrate the substrate temperature. Then, we first grew 9 nm of n.i.d. GaN, followed by a growth interruption during which we recorded the variation of the RHEED intensity over time. This first test, labeled "reference" hereafter (see black solid line in Figure 3a), served as a benchmark of the RHEED intensity transient oscillations generated by the desorption of the Ga bilayer.[47,48] Subsequently, we grew 9 nm of GaN doped with Mg using a Mg cell temperature T_{Mg} = 250 °C (see red dashed box in Figure 3b), followed by another growth interruption to monitor the intensity variation during Ga desorption (see red dashed line in Figure 3a). This second RHEED transient gives information about the perturbation introduced by the presence of Mg. If the duration and shape of this transient were similar to the "reference," it would indicate that the Mg flux neither caused a polarity inversion nor significantly altered the Ga kinetics. Conversely, a change in the desorption transient would suggest either a polarity inversion or an alteration in Ga kinetics. To discern between these possibilities, we need to regrow another layer of 9 nm of n.i.d. GaN (see red solid box in Figure 3b),

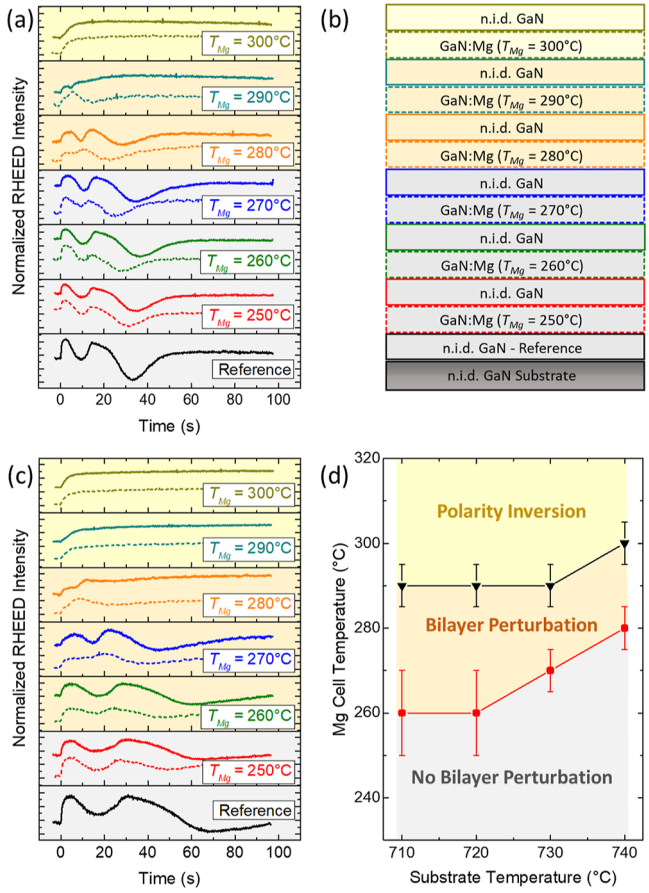

Figure 3. (a) Normalized RHEED intensity variation during the Ga desorption from n.i.d. GaN (solid lines) and from GaN:Mg at various Mg cell temperatures (dashed lines). The whole experiment was performed at T_S = 740 °C. The RHEED transients are arranged chronologically from bottom to top. (b) Schematic representation of the final sample structure obtained during the experiment described in (a). All the layers are 9 nm thick. The RHEED transients displayed in (a) were recorded during a growth interruption after the growth of each layer in (b) with the same color code and line structure (dashed and solid line for GaN:Mg and n.i.d. GaN, respectively). (c) Normalized RHEED intensity variation during the Ga desorption from n.i.d. GaN (solid lines) and from GaN:Mg (dashed lines) at T_S = 720 °C. (d) Mg cell temperatures that introduce a perturbation in the Ga bilayer and that induce a clear polarity inversion, as a function of substrate temperature.

followed by a growth interruption, which leads to the Ga desorption transient presented as a red solid line in Figure 3a. In this case, Mg is not present, meaning that any deviation in the pattern with respect to the "reference" desorption would point to an irreversible alteration of Ga kinetics on the surface, probably associated with the presence of polarity inversion domains.

In this first sequence (red transients/layers in Figure 3a,b), the deviations from the "reference" are minimum, so we can consider that the presence of Mg had little effect on the growing GaN layer from a structural point of view. Then, we increase the Mg cell temperature by 10 °C, repeat the test (green transients/layers in Figure 3a,b), and continue doing so until T_{Mg} = 300 °C.

Figure 3a illustrates the complete experiment, with the desorption transients arranged in a chronological sequence. From the bottom to the top, the figure presents the "reference," followed by the first transient after GaN:Mg growth (red dashed

https://doi.org/10.1021/acs.cgd.4c00777
Cryst. Growth Des. XXXX, XXX, XXX−XXX

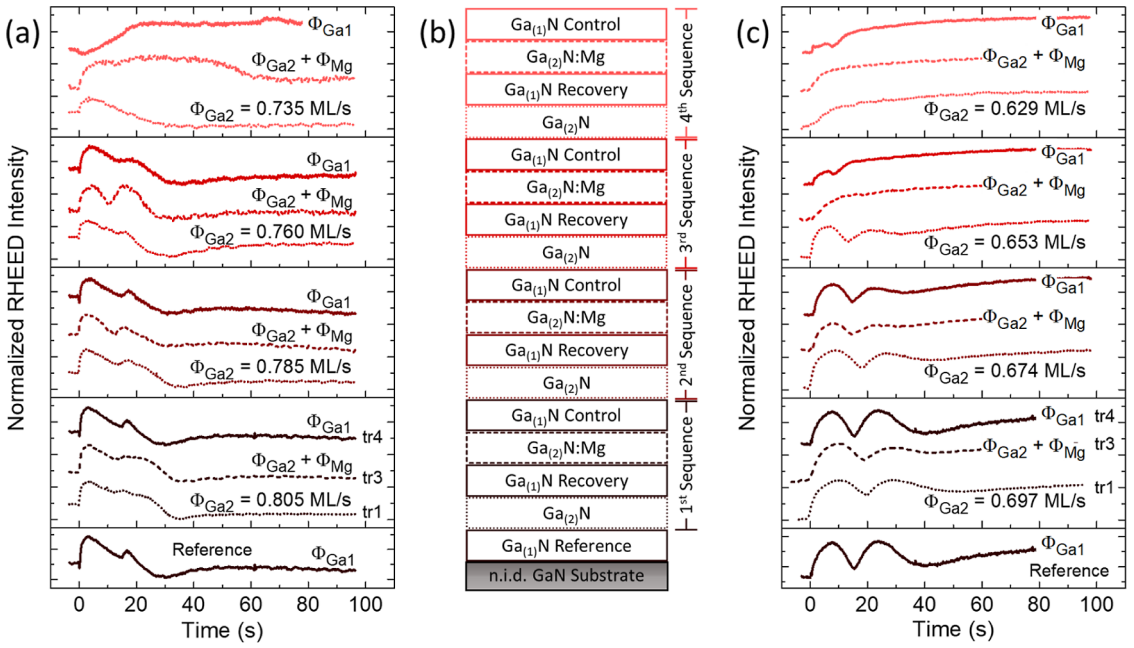

Figure 4. (a) Normalized RHEED intensity variation during Ga desorption after the growth of GaN or GaN:Mg at T_S = 740 °C, with T_{Mg} = 240 °C. The transients are arranged chronologically from bottom to top. Two Ga cells were used: the flux of Ga1 is fixed to that providing optimum growth conditions, whereas the flux of Ga2 is progressively decreased from bottom to top. The transients correspond to the initial desorption from n.i.d. GaN using Ga1 ("reference"), the desorption from n.i.d. GaN using Ga2 (tr1 and all dotted lines), the desorption from GaN:Mg using Ga2 (tr3 and all dashed lines), and the desorption from a control layer of n.i.d. GaN using Ga1 (tr4 and all solid lines). (b) Schematic representation of the final sample structure obtained during the experiment. All layers are 9 nm thick. The RHEED transients displayed in (a,c) were recorded during a growth interruption after the growth of each layer in (b) with the same color code and line structure. Each 4-layer sequence describes experiments with a fixed value of Φ_{Ga2}, which varies from sequence to sequence decreasing from bottom to top. (c) Same experiment as in (a), performed at T_S = 720 °C, with T_{Mg} = 240 °C.

line), then the transient after n.i.d. GaN (red solid line), and the subsequent repetition of these steps, each time increasing Mg cell temperature. Throughout this iterative process, the convention is maintained: dashed lines represent transients following GaN:Mg growth, and solid lines denote those following n.i.d. GaN growth. Figure 3b shows the final sample structure obtained during this experiment.

Focusing on the "reference," the bilayer desorption resulted in RHEED intensity minima is around 13 and 36 s. For low T_{Mg} values in the range of 250−270 °C, the Ga desorption from GaN:Mg is faster with respect to the reference, but the desorption after n.i.d. GaN reproduces the reference transient in both shape and duration. This indicates that Mg has an effect on the Ga kinetics, but it does not introduce a permanent structural degradation of the lattice. However, at T_{Mg} = 280 °C, the Ga desorption after n.i.d. GaN (see Figure 3a, orange solid line) also begins to accelerate, suggesting an irreversible structural perturbation that resulted in a decrease in the amount of adsorbed Ga. With a further increase of T_{Mg} to 290 °C, we observed a radical change in the desorption transient from both GaN:Mg and n.i.d. GaN, which at that point displayed only one intensity oscillation. This result indicates that nitrogen polarity is dominant. At T_{Mg} = 300 °C, the oscillations disappeared completely, which further confirms the polarity inversion. A definitive confirmation of polarity inversion was obtained upon cooling down the sample: the RHEED pattern then exhibited the characteristic 3 × 3 reconstruction associated with N-polar GaN.[49,50]

In addition to the identification of the polarity inversion point, the experiment demonstrates that Mg has a profound impact on the growth kinetics of Ga-polar GaN. The work of Northrup[36] provided a theoretical framework to understand this behavior. During growth under Mg-rich conditions, Mg atoms replace a high percentage of Ga adatoms in the structure, facilitated by the similar atomic size of Ga and Mg.[51] Surface configurations with 1/2−3/4 of Mg-substituted adatoms are particularly stable. This substitution mechanism reduces the range of Ga fluxes for which the Ga bilayer is stable and provides an explanation to the acceleration of the Ga desorption with increasing Mg flux. The accumulation of Mg on the Ga bilayer can induce a change in the stacking of the crystal structure, switching from Ga polarity to N polarity.[33]

The desorption experiment detailed previously was performed at various substrate temperatures, namely, 740 °C (Figure 3a), 730 °C, 720 °C (Figure 3c), and 710 °C. Figure 3d presents the onset of irreversible structural perturbation (acceleration of the desorption of Ga from n.i.d. GaN labeled as "bilayer perturbation") and the point where the polarity inversion domains are clearly dominant (disappearance of the Ga bilayer) for each substrate temperature. At higher substrate temperatures, the perturbation caused by Mg manifests at higher Mg cell temperatures. This can be attributed to the thermally activated nature of Mg desorption, leading to less accumulation of Mg on the surface at higher temperatures.

From these experiments, we conclude that the best strategy to enhance Mg incorporation while preventing polarity inversion is to increase the growth temperature. This not only postpones the polarity inversion but also reduces the incorporation of pollutants like oxygen and mitigates the risk of generation of nitrogen vacancies.[20] Furthermore, this experiment provides a calibration procedure for PAMBE growers to identify the Mg

https://doi.org/10.1021/acs.cgd.4c00777
Cryst. Growth Des. XXXX, XXX, XXX−XXX

temperature range that results in Ga polar GaN/Mg at a specific growth temperature in a simple and reproducible manner.

Effect of the III/V Ratio. The reproducibility issues observed around the polarity inversion threshold, particularly at high growth temperatures, prompt a closer examination of the threshold's sensitivity to the III/V ratio. To investigate this point, we have designed an experiment so that, while maintaining a constant Mg temperature, we can observe the impact of the III/V ratio on the Ga kinetics in the presence of Mg. The experiment used two Ga cells. For the first cell (Ga1), similar to the previous experiment, we selected a flux value Φ_{Ga1} slightly below Ga accumulation point (Ga cell temperature about 3 °C below the droplet formation regime). The flux Φ_{Ga1} remained constant throughout the experiment. Regarding the second cell (Ga2), starting with $\Phi_{Ga2} = \Phi_{Ga1}$, we gradually decreased Φ_{Ga2} to get access to the variation of the growth kinetics and surface structure as a function of Φ_{Ga2}. Only one cell is used at a time. Considering the diagram in Figure 3d, Mg does not significantly perturb the growth kinetics for cell temperatures lower than 250 °C. Hence, throughout this experiment, the Mg cell temperature remains constant at 240 °C for the growth of each GaN:Mg layer.

Figure 4a illustrates the complete experiment performed at T_S = 740 °C, and the final sample structure is given in Figure 4b. Here is a step-by-step breakdown of the experimental procedure.

(i) The experiment started with the deposition of 9 nm of n.i.d. GaN using Φ_{Ga1}, followed by a growth interruption during which the RHEED intensity was recorded. This RHEED transient served as a reference for the growth of GaN in optimum conditions, and it is labeled "reference" hereafter.

(ii) Then, we deposited 9 nm of n.i.d. GaN using Φ_{Ga2}, followed by a growth interruption. The resulting RHEED transient (tr1) was considered a reference for growth of GaN with a Ga flux Φ_{Ga2}.

(iii) After that, a 9 nm recovery layer of n.i.d. GaN was grown using Φ_{Ga1}. As the Φ_{Ga2} decreases along the experiment, the sample surface will no longer be flat. Hence, before depositing Mg-doped GaN layer, recovery layer is aimed at restoring a smooth GaN surface using Ga1. We measured the desorption transient (tr2, not presented here) and systematically verified that tr2 was similar to reference transient, which confirmed the recovery of the original surface quality.

(iv) The next step involves depositing a 9 nm-thick GaN:Mg layer using Φ_{Ga2}, followed by the recording of the RHEED during a growth interruption (tr3). The comparison of tr1 and tr3 provides information on the variation of the Ga kinetics due to the presence of Mg using a Ga flux = Φ_{Ga2}.

(v) To complete the sequence, a 9 nm-thick n.i.d. GaN control layer is deposited using Φ_{Ga1}, followed by a growth interruption (tr4). The comparison of tr2 and tr4 tells us if Mg has introduced a permanent structural change and allows the eventual identification of a polarity inversion. The loop is completed by decreasing Φ_{Ga2} by around 3% and retaking the sequence in step (ii).

Note that in Figure 4a, the desorption transients are arranged in a chronological sequence, extending from the bottom to top. For simplicity, we have represented only tr1 (dotted lines, Ga desorption from n.i.d. GaN grown using Φ_{Ga2}), tr3 (dashed lines, Ga desorption from GaN:Mg grown using Φ_{Ga2}), and tr4 (solid lines, Ga desorption from n.i.d. GaN grown using Φ_{Ga1}). The tr2 transients are not shown in the figure since they were systematically identical to tr4 of the previous sequence.

Starting at Φ_{Ga2} = 0.805 ML/s and comparing tr1 and tr3, there is no discernible impact of Mg on the desorption time of Ga. Also comparing tr4 and the "reference" transient, the growth of the GaN:Mg did not perturb the GaN structure. As the Ga2 flux decreases to Φ_{Ga2} = 0.785 ML/s, the shape of tr3 confirms that we are still in the Ga bilayer regime, but the transient is slightly faster than in the previous series, confirming that there is less Ga in the bilayer. Nevertheless, comparing tr1 and tr3, and also tr4 and "reference," the presence of Mg in the GaN:Mg layer did not introduce any perturbation. The same conclusions can be extracted from the transients at Φ_{Ga2} = 0.760 ML/s. However, major changes occurred at an Φ_{Ga2} of 0.735 ML/s. Here, the shape of tr1 suggests that we had only one layer of Ga excess when growing n.i.d. GaN. The bilayer was recovered during the growth with Ga1 (tr2, not shown). The transient after growth of GaN:Mg with Ga2 (tr3) also exhibits only a monolayer. After the deposition of this GaN:Mg layer, attempts to grow n.i.d. GaN using Ga1 failed to restore the Ga bilayer, which indicates that a polarity inversion took place.

From this experiment, we conclude that a Ga excess of only one monolayer of Ga is insufficient to prevent polarity inversion. Hence, maintaining growth within the bilayer regime is critical for the successful synthesis of Mg-doped Ga-polar GaN, which outlines the critical balance required in the Ga flux to safeguard the structural quality of the material.

In Figure 4c, the same experiment performed at T_S = 720 °C is presented to investigate the influence of the substrate temperature. At this substrate temperature, the optimum growth conditions correspond to an Φ_{Ga1} of 0.697 ML/s. Note that the Ga flux values vary depending on the substrate temperature since evaporation rate of Ga differs. The temperature of the Mg cell was 240 °C, the same as in the previous experiment.

At high Ga2 fluxes (Φ_{Ga2} = 0.697 ML/s), the desorption transients present the behavior of the desorption of the Ga bilayer, even in the presence of Mg. Decreasing to Φ_{Ga2} = 0.674 ML/s, Mg begins to exert its effect, accelerating the Ga desorption in the case of GaN:Mg growth (dashed line) with respect to n.i.d. growth (dotted line). The structural perturbation introduced by Mg is irreversible, since the desorption transient after growth with Ga1 is also accelerated (solid line, to be compared with tr4 of the previous sequence). Then, when the Ga2 flux is set to Φ_{Ga2} = 0.653 ML/s, the bilayer disappears during the growth of GaN:Mg (dashed line), and it is not recovered during the growth of the control layer with Ga1 flux (solid line), which confirms that the polarity of the layer is inverted. The inversion is further confirmed by looking at the desorption transients in the sequence with Φ_{Ga2} = 0.629 ML/s.

Comparing the experiments in Figure 4a,c, we realize that at 720 °C, the effect of Mg appears earlier: there are signs of partial (perturbation of the bilayer) and complete polarity inversion still in the presence of a Ga bilayer (Φ_{Ga2} = 0.674 ML/s and Φ_{Ga2} = 0.653 ML/s, respectively, in Figure 4c). The variation in behavior can be attributed to the faster evaporation of Mg at higher substrate temperatures. Consequently, the substitution of Ga atoms by Mg in the bilayer is delayed at higher temperatures, reducing the probability of polarity inversion. These observations are consistent with Figure 3c, as it indicates that the perturbation of the Ga bilayer is more pronounced at lower substrate temperatures and it is observed for a larger range of Mg cell temperatures before reaching the polarity inversion threshold. In contrast, at higher substrate temperatures, the

https://doi.org/10.1021/acs.cgd.4c00777
Cryst. Growth Des. XXXX, XXX, XXX−XXX

bilayer perturbation and polarity inversion occur in close proximity to each other.

DISCUSSION

Our experiments describe how Mg significantly influences Ga-polar GaN growth kinetics, replacing a high percentage of Ga adatoms under Mg-rich conditions and thereby affecting the stability of the Ga bilayer. This substitution accelerates Ga desorption with increasing Mg flux, thereby narrowing the range of Ga fluxes, sustaining bilayer stability. We observe that the disappearance of the bilayer under the influence of Mg prompts polarity inversion.

Analyzing the experiments conducted at various substrate temperatures, it is evident that higher substrate temperatures delay polarity inversion, offering a strategic approach to enhance Mg incorporation without compromising the structural integrity of GaN. On the other hand, experiments performed with different Ga fluxes highlight the critical balance required in Ga flux to maintain the bilayer regime when Mg is present, which is essential to prevent polarity inversion. A decrease of the Ga flux by 7% (9%) can lead to polarity inversion at T_S = 720 °C (T_S = 740 °C). It is hence important to ensure that the growth of the Mg-doped layer takes place under an important Ga excess, not only within the bilayer regime but also close to the threshold of accumulation of Ga droplets. In this sense, our experimental observations contradict some reports in the literature that suggest that the presence of the Ga bilayer inhibits Mg incorporation.[52−54]

CONCLUSIONS

In conclusion, our experiments provide several important insights into how the substrate temperature and III/V ratio influence the synthesis of GaN:Mg by PAMBE. At relatively low substrate temperatures (650 °C in our experiments), where Ga desorption is minimal, a self-compensating effect associated with polarity inversion causes a collapse in net acceptor concentration at relatively low Mg cell temperatures. Higher substrate temperatures enable the use of higher Mg fluxes to attain an increased net acceptor concentration before such collapse. However, reproducibility issues emerge at high Mg cell temperatures, and polarity inversion is still the limiting factor to achieving higher Mg doping levels.

To further explore the effect of Mg on the growth kinetics and identify precisely the conditions leading to polarity inversion, we have designed experiments based on analysis of the Ga desorption during growth interruptions. We show that the Ga bilayer can be perturbed and even inhibited in the presence of the Mg flux, a phenomenon attributed to Mg atoms replacing a large number of Ga adatoms, thus compromising the stability of the Ga bilayer. When the Mg flux is high enough to force the disappearance of the Ga bilayer, polarity inversion occurs. The process is also highly sensitive to Ga flux. Consequently, it is important to ensure that the growth of the Mg-doped layer takes place under an important Ga excess, within the bilayer regime, yet closely approaching the threshold of accumulation of Ga droplets, to reduce the risk of polarity inversion.

ASSOCIATED CONTENT

Supporting Information

The Supporting Information is available free of charge at https://pubs.acs.org/doi/10.1021/acs.cgd.4c00777.

SEM and BF-STEM images of the sample with polarity inversion (PDF)

AUTHOR INFORMATION

Corresponding Author

Elçin Akar − *CEA, Grenole INP, IRIG, PHELIQS, Univ. Grenoble-Alpes, 38000 Grenoble, France;* orcid.org/0009-0002-4221-3357; Email: elcin.akar@cea.fr

Authors

Adeline Grenier − *CEA, LETI, Univ. Grenoble-Alpes, 38000 Grenoble, France*

Anne-Marie Papon − *CEA, LETI, Univ. Grenoble-Alpes, 38000 Grenoble, France*

Audrey Jannaud − *CEA, LETI, Univ. Grenoble-Alpes, 38000 Grenoble, France*

Martien Ilse den Hertog − *CNRS, Grenoble INP, Institut Néel, Univ. Grenoble-Alpes, 38000 Grenoble, France;* orcid.org/0000-0003-0781-9249

Eva Monroy − *CEA, Grenole INP, IRIG, PHELIQS, Univ. Grenoble-Alpes, 38000 Grenoble, France;* orcid.org/0000-0001-5481-3267

Complete contact information is available at: https://pubs.acs.org/10.1021/acs.cgd.4c00777

Notes

The authors declare no competing financial interest.

ACKNOWLEDGMENTS

The authors would like to thank Yoann Curé, Fabien Jourdan, and Yann Genuist for their technical support. This work received funding from the European Research Council under the European Union's H2020 Research and Innovation programme via the e-See project (grant no. 758385) and from the French National Research Agency (ANR) via the INMOST project (ANR-19-CE08-0025).

REFERENCES

(1) Malinverni, M.; Martin, D.; Grandjean, N. InGaN Based Micro Light Emitting Diodes Featuring a Buried GaN Tunnel Junction. *Appl. Phys. Lett.* **2015**, *107* (5), 051107.

(2) Lee, S.; Forman, C. A.; Kearns, J.; Leonard, J. T.; Cohen, D. A.; Nakamura, S.; DenBaars, S. P. Demonstration of GaN-Based Vertical-Cavity Surface-Emitting Lasers with Buried Tunnel Junction Contacts. *Opt. Express* **2019**, *27* (22), 31621.

(3) Ji, D.; Chowdhury, S. On the Scope of GaN-Based Avalanche Photodiodes for Various Ultraviolet-Based Applications. *Front. Mater.* **2022**, *9*..

(4) Hautakangas, S.; Oila, J.; Alatalo, M.; Saarinen, K.; Liszkay, L.; Seghier, D.; Gislason, H. P. Vacancy Defects as Compensating Centers in Mg-Doped GaN. *Phys. Rev. Lett.* **2003**, *90* (13), 137402.

(5) Miceli, G.; Pasquarello, A. Self-Compensation Due to Point Defects in Mg-Doped GaN. *Phys. Rev. B* **2016**, *93*, 165207.

(6) Buckeridge, J.; Catlow, C. R. A.; Scanlon, D. O.; Keal, T. W.; Sherwood, P.; Miskufova, M.; Walsh, A.; Woodley, S. M.; Sokol, A. A. Determination of the Nitrogen Vacancy as a Shallow Compensating Center in GaN Doped with Divalent Metals. *Phys. Rev. Lett.* **2015**, *114* (1), 016405.

(7) Yan, Q.; Janotti, A.; Scheffler, M.; Van De Walle, C. G. Role of Nitrogen Vacancies in the Luminescence of Mg-Doped GaN. *Appl. Phys. Lett.* **2012**, *100* (14), 142110.

(8) Liang, Y.-H.; Towe, E. Progress in Efficient Doping of High Aluminum-Containing Group III-Nitrides. *Appl. Phys. Rev.* **2018**, *5* (1), 011107.

(9) Wu, Y.; Liu, B.; Xu, F.; Sang, Y.; Tao, T.; Xie, Z.; Wang, K.; Xiu, X.; Chen, P.; Chen, D.; Lu, H.; Zhang, R.; Zheng, Y. High-Efficiency Green Micro-LEDs with GaN Tunnel Junctions Grown Hybrid by PA-MBE and MOCVD. *Photonics Res.* **2021**, *9* (9), 1683.
(10) Young, E. C.; Yonkee, B. P.; Wu, F.; Oh, S. H.; DenBaars, S. P.; Nakamura, S.; Speck, J. S. Hybrid Tunnel Junction Contacts to III-Nitride Light-Emitting Diodes. *Appl. Phys. Express* **2016**, *9* (2), 022102.
(11) Wong, M. S.; Speck, J. S.; Nakamura, S.; DenBaars, S. P. Progress in III-Nitride Tunnel Junctions for Optoelectronic Devices. *IEEE J. Quantum Electron.* **2022**, *58* (4), 1−11.
(12) Namkoong, G.; Trybus, E.; Lee, K. K.; Moseley, M.; Doolittle, W. A.; Look, D. C. Metal Modulation Epitaxy Growth for Extremely High Hole Concentrations above 1019 cm-3 in GaN. *Appl. Phys. Lett.* **2008**, *93* (17), 172112.
(13) Gunning, B. P.; Fabien, C. A. M.; Merola, J. J.; Clinton, E. A.; Doolittle, W. A.; Wang, S.; Fischer, A. M.; Ponce, F. A. Comprehensive Study of the Electronic and Optical Behavior of Highly Degenerate P-Type Mg-Doped GaN and AlGaN. *J. Appl. Phys.* **2015**, *117* (4), 045710.
(14) Kyle, E. C. H.; Kaun, S. W.; Young, E. C.; Speck, J. S. Increased P-Type Conductivity through Use of an Indium Surfactant in the Growth of Mg-Doped GaN. *Appl. Phys. Lett.* **2015**, *106* (22), 222103.
(15) Zhang, K.; Liang, H.; Shen, R.; Song, S.; Wang, D.; Liu, Y.; Xia, X.; Yang, D.; Luo, Y.; Du, G. Smooth Surface Morphology and Low Dislocation Density of P-GaN Using Indium-Assisted Growth. *Appl. Phys. A: Mater. Sci. Process.* **2014**, *116* (4), 1561−1566.
(16) Chen, Y.; Wu, H.; Yue, G.; Chen, Z.; Zheng, Z.; Wu, Z.; Wang, G.; Jiang, H. Enhanced Mg Doping Efficiency in P-Type GaN by Indium-Surfactant-Assisted Delta Doping Method. *Appl. Phys. Express* **2013**, *6* (4), 041001.
(17) Guha, S.; Bojarczuk, N. A.; Cardone, F. Mg in GaN: Incorporation of a Volatile Species at High Temperatures during Molecular Beam Epitaxy. *Appl. Phys. Lett.* **1997**, *71* (12), 1685−1687.
(18) Ptak, A. J.; Myers, T. H.; Romano, L. T.; Van de Walle, C. G.; Northrup, J. E. Magnesium Incorporation in GaN Grown by Molecular-Beam Epitaxy. *Appl. Phys. Lett.* **2001**, *78* (3), 285−287.
(19) Haus, E.; Smorchkova, I. P.; Heying, B.; Fini, P.; Poblenz, C.; Mates, T.; Mishra, U. K.; Speck, J. S. The Role of Growth Conditions on the P-Doping of GaN by Plasma-Assisted Molecular Beam Epitaxy. *J. Cryst. Growth* **2002**, *246*, 55−63.
(20) Feduniewicz, A.; Skierbiszewski, C.; Siekacz, M.; Wasilewski, Z. R.; Sproule, I.; Grzanka, S.; Jakieła, R.; Borysiuk, J.; Kamler, G.; Litwin-Staszewska, E.; Czernecki, R.; Boćkowski, M.; Porowski, S. Control of Mg Doping of GaN in RF-Plasma Molecular Beam Epitaxy. *J. Cryst. Growth* **2005**, *278* (1−4), 443−448.
(21) Monroy, E.; Andreev, T.; Holliger, P.; Bellet-Amalric, E.; Shibata, T.; Tanaka, M.; Daudin, B. Modification of GaN(0001) Growth Kinetics by Mg Doping. *Appl. Phys. Lett.* **2004**, *84* (14), 2554−2556.
(22) Smorchkova, I. P.; Haus, E.; Heying, B.; Kozodoy, P.; Fini, P.; Ibbetson, J. P.; Keller, S.; DenBaars, S. P.; Speck, J. S.; Mishra, U. K. Mg Doping of GaN Layers Grown by Plasma-Assisted Molecular-Beam Epitaxy. *Appl. Phys. Lett.* **2000**, *76* (6), 718−720.
(23) Green, D. S.; Haus, E.; Wu, F.; Chen, L.; Mishra, U. K.; Speck, J. S. Polarity Control during Molecular Beam Epitaxy Growth of Mg-Doped GaN. *J. Vac. Sci. Technol., B: Microelectron. Nanometer Struct.* **2003**, *21* (4), 1804−1811.
(24) Vennéguès, P.; Benaissa, M.; Beaumont, B.; Feltin, E.; De Mierry, P.; Dalmasso, S.; Leroux, M.; Gibart, P. Pyramidal Defects in Metalorganic Vapor Phase Epitaxial Mg Doped GaN. *Appl. Phys. Lett.* **2000**, *77* (6), 880−882.
(25) Leroux, M.; Vennéguès, P.; Dalmasso, S.; Benaissa, M.; Feltin, E.; de Mierry, P.; Beaumont, B.; Damilano, B.; Grandjean, N.; Gibart, P. Structural Defects and Relation with Optoelectronic Properties in Highly Mg-Doped GaN. *Phys. Status Solidi A* **2002**, *192* (2), 394−400.
(26) Pezzagna, S.; Vennéguès, P.; Grandjean, N.; Massies, J. Polarity Inversion of GaN(0001) by a High Mg Doping. *J. Cryst. Growth* **2004**, *269* (2−4), 249−256.
(27) Stutzmann, M.; Ambacher, O.; Eickhoff, M.; Karrer, U.; Lima Pimenta, A.; Neuberger, R.; Schalwig, J.; Dimitrov, R.; Schuck, P. J.; Grober, R. D. Playing with Polarity. *Phys. Status Solidi B* **2001**, *228* (2), 505−512.
(28) Kim, E.; Zhang, Z.; Encomendero, J.; Singhal, J.; Nomoto, K.; Hickman, A.; Wang, C.; Fay, P.; Toita, M.; Jena, D.; Xing, H. G. N-Polar GaN/AlGaN/AlN High Electron Mobility Transistors on Single-Crystal Bulk AlN Substrates. *Appl. Phys. Lett.* **2023**, *122* (9), 092104.
(29) Li, L. K.; Jurkovic, M. J.; Wang, W. I.; Van Hove, J. M.; Chow, P. P. Surface Polarity Dependence of Mg Doping in GaN Grown by Molecular-Beam Epitaxy. *Appl. Phys. Lett.* **2000**, *76* (13), 1740−1742.
(30) Kandaswamy, P. K.; Guillot, F.; Bellet-Amalric, E.; Monroy, E.; Nevou, L.; Tchernycheva, M.; Michon, A.; Julien, F. H.; Baumann, E.; Giorgetta, F. R.; Hofstetter, D.; Remmele, T.; Albrecht, M.; Birner, S.; Dang, L. S. GaN/AlN Short-Period Superlattices for Intersubband Optoelectronics: A Systematic Study of Their Epitaxial Growth, Design, and Performance. *J. Appl. Phys.* **2008**, *104* (9), 093501.
(31) Valdueza-Felip, S.; Bellet-Amalric, E.; Núñez-Cascajero, A.; Wang, Y.; Chauvat, M.-P.; Ruterana, P.; Pouget, S.; Lorenz, K.; Alves, E.; Monroy, E. High In-Content InGaN Layers Synthesized by Plasma-Assisted Molecular-Beam Epitaxy: Growth Conditions, Strain Relaxation, and In Incorporation Kinetics. *J. Appl. Phys.* **2014**, *116* (23), 233504.
(32) Qi, H. R.; Zhang, S.; Liu, S. T.; Liang, F.; Yi, L. K.; Huang, J. L.; Zhou, M.; He, Z. W.; Zhao, D. G.; Jiang, D. S. The Self-Compensation Effect of Heavily Mg Doped p-GaN Films Studied by SIMS and Photoluminescence. *Superlattices Microstruct.* **2019**, *133*, 106177.
(33) Ramachandran, V.; Feenstra, R. M.; Sarney, W. L.; Salamanca-Riba, L.; Northrup, J. E.; Romano, L. T.; Greve, D. W. Inversion of Wurtzite GaN(0001) by Exposure to Magnesium. *Appl. Phys. Lett.* **1999**, *75* (6), 808−810.
(34) Northrup, J. E. Magnesium Incorporation at (0001) Inversion Domain Boundaries in GaN. *Appl. Phys. Lett.* **2003**, *82* (14), 2278−2280.
(35) Romano, L. T.; Northrup, J. E.; Ptak, A. J.; Myers, T. H. Faceted Inversion Domain Boundary in GaN Films Doped with Mg. *Appl. Phys. Lett.* **2000**, *77* (16), 2479−2481.
(36) Northrup, J. E. Effect of Magnesium on the Structure and Growth of GaN(0001). *Appl. Phys. Lett.* **2005**, *86* (12), 122108.
(37) Sheikhi, M.; Li, J.; Meng, F.; Li, H.; Guo, S.; Liang, L.; Cao, H.; Gao, P.; Ye, J.; Guo, W. Polarity Control of GaN and Realization of GaN Schottky Barrier Diode Based on Lateral Polarity Structure. *IEEE Trans. Electron Devices* **2017**, *64* (11), 4424−4429.
(38) Weyher, J. L.; van Dorp, D. H.; Conard, T.; Nowak, G.; Levchenko, I.; Kelly, J. J. Chemical Etching of GaN in KOH Solution: Role of Surface Polarity and Prior Photoetching. *J. Phys. Chem. C* **2022**, *126* (2), 1115−1124.
(39) Koblmüller, G.; Brown, J.; Averbeck, R.; Riechert, H.; Pongratz, P.; Speck, J. S. Ga Adlayer Governed Surface Defect Evolution of (0001)GaN Films Grown by Plasma-Assisted Molecular Beam Epitaxy. *Jpn. J. Appl. Phys.* **2005**, *44*, 906−908.
(40) Huang, D.; Reshchikov, M. A.; Visconti, P.; Yun, F.; Baski, A. A.; King, T.; Morkoç, H.; Jasinski, J.; Liliental-Weber, Z.; Litton, C. W. Comparative Study of Ga- and N-Polar GaN Films Grown on Sapphire Substrates by Molecular Beam Epitaxy. *J. Vac. Sci. Technol., B: Microelectron. Nanometer Struct.* **2002**, *20* (6), 2256−2264.
(41) Masui, H.; Keller, S.; Fellows, N.; Fichtenbaum, N. A.; Furukawa, M.; Nakamura, S.; Mishra, U. K.; DenBaars, S. P. Luminescence Characteristics of N-Polar GaN and InGaN Films Grown by Metal Organic Chemical Vapor Deposition. *Jpn. J. Appl. Phys.* **2009**, *48*, 071003.
(42) Chèze, C.; Feix, F.; Lähnemann, J.; Flissikowski, T.; Kryśko, M.; Wolny, P.; Turski, H.; Skierbiszewski, C.; Brandt, O. Luminescent N-polar (In,Ga)N/GaN quantum wells achieved by plasma-assisted molecular beam epitaxy at temperatures exceeding 700 °C. *Appl. Phys. Lett.* **2018**, *112* (2), 022102.
(43) Monroy, E.; Sarigiannidou, E.; Fossard, F.; Gogneau, N.; Bellet-Amalric, E.; Rouvière, J. L.; Monnoye, S.; Mank, H.; Daudin, B. Growth Kinetics of N-Face Polarity GaN by Plasma-Assisted Molecular-Beam Epitaxy. *Appl. Phys. Lett.* **2004**, *84* (18), 3684−3686.

https://doi.org/10.1021/acs.cgd.4c00777
Cryst. Growth Des. XXXX, XXX, XXX−XXX

(44) Northrup, J.; Neugebauer, J.; Feenstra, R.; Smith, A. Structure of GaN(0001): The Laterally Contracted Ga Bilayer Model. *Phys. Rev. B* **2000**, *61* (15), 9932−9935.
(45) Adelmann, C.; Brault, J.; Jalabert, D.; Gentile, P.; Mariette, H.; Mula, G.; Daudin, B. Dynamically Stable Gallium Surface Coverages during Plasma-Assisted Molecular-Beam Epitaxy of (0001) GaN. *J. Appl. Phys.* **2002**, *91* (12), 9638−9645.
(46) Kaufmann, N. A. K.; Lahourcade, L.; Hourahine, B.; Martin, D.; Grandjean, N. Critical Impact of Ehrlich-Schwöbel Barrier on GaN Surface Morphology during Homoepitaxial Growth. *J. Cryst. Growth* **2016**, *433*, 36−42.
(47) Heying, B.; Averbeck, R.; Chen, L. F.; Haus, E.; Riechert, H.; Speck, J. S. Control of GaN Surface Morphologies Using Plasma-Assisted Molecular Beam Epitaxy. *J. Appl. Phys.* **2000**, *88* (4), 1855−1860.
(48) Adelmann, C.; Brault, J.; Mula, G.; Daudin, B.; Lymperakis, L.; Neugebauer, J. Gallium Adsorption on (0001) GaN Surfaces. *Phys. Rev. B* **2003**, *67* (16), 165419.
(49) Hughes, O. H.; Cheng, T. S.; Novikov, S. V.; Foxon, C. T.; Korakakis, D.; Jeffs, N. RHEED Studies of the GaN Surface during Growth by Molecular Beam Epitaxy. *J. Cryst. Growth* **1999**, *201−202*, 388−391.
(50) Smith, A. R.; Feenstra, R. M.; Greve, D. W.; Neugebauer, J.; Northrup, J. E. Reconstructions of the GaN (000 1^{-}) Surface. *Phys. Rev. Lett.* **1997**, *79* (20), 3934−3937.
(51) Rahm, M.; Hoffmann, R.; Ashcroft, N. W. Atomic and Ionic Radii of Elements 1−96. *Chem. −Eur. J.* **2016**, *22*, 14625−14632.
(52) Tang, H.; Sadaf, S. M.; Wu, X.; Jiang, W. Highly Efficient P-Type Doping of GaN under Nitrogen-Rich and Low-Temperature Conditions by Plasma-Assisted Molecular Beam Epitaxy. *AIP Adv.* **2019**, *9* (5), 055008.
(53) Sadaf, S. Md.; Tang, H. Mapping the Growth of *p* -Type GaN Layer under Ga-Rich and N-Rich Conditions at Low to High Temperatures by Plasma-Assisted Molecular Beam Epitaxy. *Appl. Phys. Lett.* **2020**, *117* (25), 254104.
(54) Zhang, M.; Bhattacharya, P.; Guo, W.; Banerjee, A. Mg Doping of GaN Grown by Plasma-Assisted Molecular Beam Epitaxy under Nitrogen-Rich Conditions. *Appl. Phys. Lett.* **2010**, *96* (13), 132103.

https://doi.org/10.1021/acs.cgd.4c00777
Cryst. Growth Des. XXXX, XXX, XXX−XXX